Available online at www.sciencedirect.com
SCIENCE DIRECT
Journal of Molecular Graphics and Modelling 24 (2006) 373–382
Journal of Molecular Graphics and Modelling
www.elsevier.com/locate/JMGM

Adsorption and diffusion of benzene in the nanoporous catalysts FAU, ZSM-5 and MCM-22: A molecular dynamics study

Ratana Rungsirisakun [a], Tanin Nanok [a], Michael Probst [c], Jumras Limtrakul [a,b,*]

[a] *Laboratory for Computational and Applied Chemistry, Physical Chemistry Division, Department of Chemistry, Faculty of Science, Kasetsart University, Bangkok 10900, Thailand*
[b] *Center of Nanotechnology, Kasetsart University Research and Development Institute, Bangkok 10900, Thailand*
[c] *Institut für Ionenphysik, Universität Innsbruck, Technikerstraße 25, 6020 Innsbruck, Austria*

Received 17 August 2005; accepted 7 October 2005
Available online 9 November 2005

Abstract

Molecular dynamics (MD) simulations of benzene in siliceous zeolites (FAU, ZSM-5, and MCM-22) were performed at loadings of 1, 2, 4, 8, and 16 molecules per supercell. The potential energy functions for these simulations were constructed in a semi-empirical way from existing potentials and experimental energetic data. The MD simulations were employed to analyze the dynamic properties of the benzene–zeolite systems. The adsorption energies of benzene/siliceous zeolite complexes increase with increasing loading number, due to the intermolecular attraction between benzene molecules. The self-diffusion coefficient of benzene in siliceous zeolites decreases with increasing loading due to the steric hindrance between the sorbates passing each other. From the zeolite–benzene radial distribution functions it was found that the benzene molecules are relatively far from each other, about 5.2 Å for siliceous FAU, 5.2 Å for siliceous ZSM-5, and 4.8 Å for siliceous MCM-22. In the case of FAU, the benzene molecules prefer to be adsorbed parallel to the surface of the sodalite cage above the six-membered-ring. In ZSM-5, we found a T-structure of the benzene molecules at loadings 2, 4, and 8 molecules per supercell. At loadings of 16 molecules per supercell, the molecules are lined up along the straight channel and their movement is highly correlated. For MCM-22 we found adjacent benzene molecules at a loading of 4 molecules with an orientation similar to the stacked conformation of benzene dimer in the gas phase.

Keywords: Molecular dynamics; FAU; ZSM-5; MCM-22; Benzene; Adsorption; Diffusion

1. Introduction

Zeolites are porous crystals with a wide range of applications in the chemical and petroleum industry as catalysts, molecular sieves and sorbents [1,2]. For these applications, the diffusion of sorbate molecules through the pores within the crystals determines, to a large extent, the mechanisms of catalysis and adsorption in these materials since the sorbates have to travel through the channel system before reaction can occur at the active site [3]. The diffusion of aromatic hydrocarbons in siliceous zeolites is interesting because several petrochemical processes involve the transformation of aromatic molecules within the pores of zeolites [3].

ZSM-5 and FAU zeolites have been proven to catalyze the synthesis of cumene, $C_6H_5(CH)(CH_3)_2$, by the alkylation of benzene with propylene [4]. The product, cumene, can then be converted to phenol and acetone by peroxidation. The former is an important petrochemical used in the phenolic resins, nylon, and many other chemicals [5,6]. A new high silica zeolite, MCM-22, has also been claimed to be a good catalysts for cumene synthesis [7–9]. It is, therefore, interesting to investigate the adsorption and diffusion of aromatic hydrocarbons within the pores of such siliceous zeolites. The adsorption of molecules can be studied experimentally, for example, by vibrational spectroscopy. However, vibrational spectra of zeolites (or other porous materials) are normally difficult to interpret. Moreover, details of the diffusion process are very difficult to obtain from experiments. Atomistic molecular dynamics (MD) simulations based on analytical potential functions provide a way to study the microscopic details of such processes. They have proven to be effective in modeling the diffusion of organic molecules in zeolites [10–12].

In this work, the diffusion of aromatic molecules in the pores of siliceous FAU, ZSM-5, and MCM-22 with different sizes has

* Corresponding author. Tel.: +66 2 942 8900x323; fax: +66 2 942 8900x324.
E-mail address: fscijrl@ku.ac.th (J. Limtrakul).

1093-3263/$ – see front matter © 2005 Elsevier Inc. All rights reserved.
doi:10.1016/j.jmgm.2005.10.003

been studied by MD simulations. The aim of this investigation is to understand the diffusion behavior in terms of the relative sizes of the sorbate and the channel system at different loadings. The reliability of results obtained from MD simulations depends strongly on the potential functions used [13]. We present parameters of potential functions which we believe to be appropriate to describe the interactions between siliceous FAU, ZSM-5 and MCM-22 and benzene. Adsorption energies and diffusion coefficients of benzene in these zeolites at different loadings have been calculated from the simulated trajectories and are compared with experimental results.

2. Methodology

2.1. Structures of siliceous FAU, ZSM-5 and MCM-22

The structure of FAU was taken from X-ray and neutron powder diffraction data [14,15]. The framework is composed of cubooctahedral sodalite cages linked together in a tetrahedral arrangement by six-membered rings of O atoms to form a large cavity, called supercage [16]. The supercages are interconnected by 12-membered ring windows. The unit cell of FAU is cubic ($a = b = c = 24.20$ Å) and comprises of eight sodalite cages and eight supercages. Each unit cell contains 192 Si atoms and 384 O atoms (Fig. 1a).

ZSM-5 is a zeolite which contains a network of interconnected straight and zigzag channels. The unit cell of ZSM-5 is orthorhombic, with $a = 20.02$ Å, $b = 19.98$ Å, and $c = 13.38$ Å. One unit cell of ZSM-5 contains 288 atoms (96 Si atoms and 192 O atoms). In the present work, the simulation cell consists of two unit cells in the c-direction which contains a complete intersecting channel of ZSM-5 (Fig. 2a).

MCM-22 is a molecular sieve with a unique structure [17]. Its framework has been derived from high-resolution electron micrographs and synchrotron X-ray diffraction power data. The framework comprises of two independent pore systems, both accessible through a 10-membered ring window. One of these pore systems is two-dimensional and the other consists of large supercages made up from 12-membered rings with a free diameter of 7.1 Å and an inner height of 18.2 Å [17,18]. The unit cell is hexagonal and consists of 216 atoms. In the simulation we used an orthorhombic supercell containing 864 atoms (288 Si atoms and 576 O atoms; $a = 24.42$ Å, $b = 28.19$ Å, and $c = 24.84$ Å). It is shown in Fig. 3a.

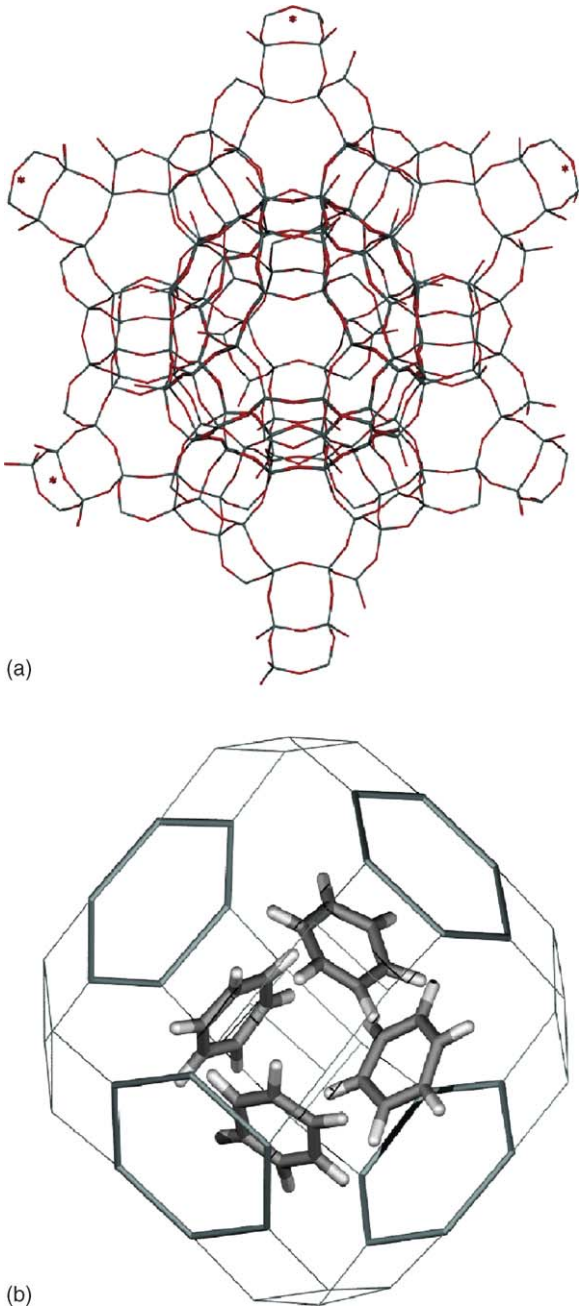

Fig. 1. Schematic view of: (a) the structure of FAU showing the supercage of FAU zeolite in the unit cell; (b) a snapshot of four benzene molecules in one supercage.

2.2. Potential parameters

The total potential energy of the zeolite–benzene complex consists of four terms in the potential function:

$$V_{\text{total}} = V_{\text{zeolite}} + V_{\text{benzene}} + V_{\text{benzene-benzene}} + V_{\text{zeolite-benzene}} \quad (1)$$

where V_{zeolite} is the intramolecular potential energy of zeolite, V_{benzene} is the intramolecular potential energy of benzene, $V_{\text{benzene-benzene}}$ is the potential energy between benzene molecules and $V_{\text{zeolite-benzene}}$ is the potential energy between the benzene molecules and the zeolitic wall. The mathematical expressions used in the potential functions are shown in Table 1.

The potential energy functions V_{zeolite} of FAU, ZSM-5, and MCM-22 frameworks are taken from the work of Nicholas et al. [19] in which the Si–O bond stretches and the O–Si–O bond bends are represented by simple harmonic potentials and the Si–O–Si bond bends are represented by a quartic potential. The equilibrium values for bond distances and bond angles, r_0 and θ_0, are taken from the work of Smirnov and Bougeard [20].

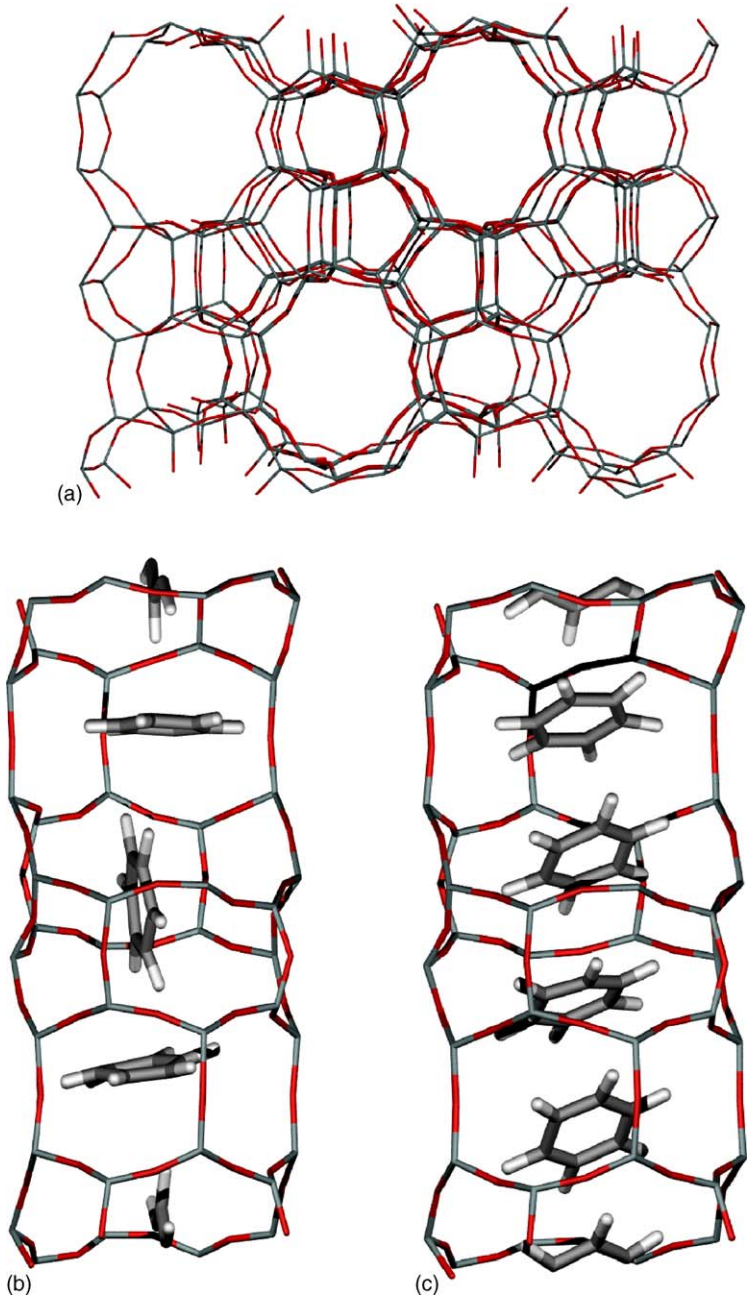

Fig. 2. Schematic view of: (a) the structure of ZSM-5 zeolites showing a network of interconnected straight and zigzag channels; (b) a snapshot of the distribution of four benzene molecules; (c) a snapshot of the distribution of benzene molecules at loadings of 16 molecules per supercell in the straight channel. The molecules are lined up along the straight channel.

Table 1
Types of interaction potentials and mathematical expression used in the analytical potentials

Type of term	Expression	Used in
Harmonic stretching	$V_{\text{two-body}} = \frac{1}{2}k(r - r_0)^2$	V_{zeolite}, V_{benzene}
Harmonic bending	$V_{\text{three-body}} = \frac{1}{2}k(\theta - \theta_0)^2$	V_{zeolite}, V_{benzene}
Quartic bending	$V_{\text{three-body}} = \frac{k}{2}(\theta - \theta_0)^2 + \frac{k'}{3}(\theta - \theta_0)^3 + \frac{k''}{4}(\theta - \theta_0)^4$	V_{zeolite}
Bond torsion	$V_{\text{four-body}} = A[1 + \cos(m\phi - \delta)]$	V_{benzene}
Lennard–Jones	$V_{\text{Lennard–Jones}} = 4\varepsilon\left[\left(\frac{\sigma}{r_{ij}}\right)^{12} - \left(\frac{\sigma}{r_{ij}}\right)^{6}\right]$	V_{benzene}, $V_{\text{benzene–benzene}}$, $V_{\text{zeolite–benzene}}$
Coulomb	$V_{\text{coul}} = \frac{q_i q_j}{r_{ij}}$	$V_{\text{benzene–benzene}}$, $V_{\text{zeolite–benzene}}$

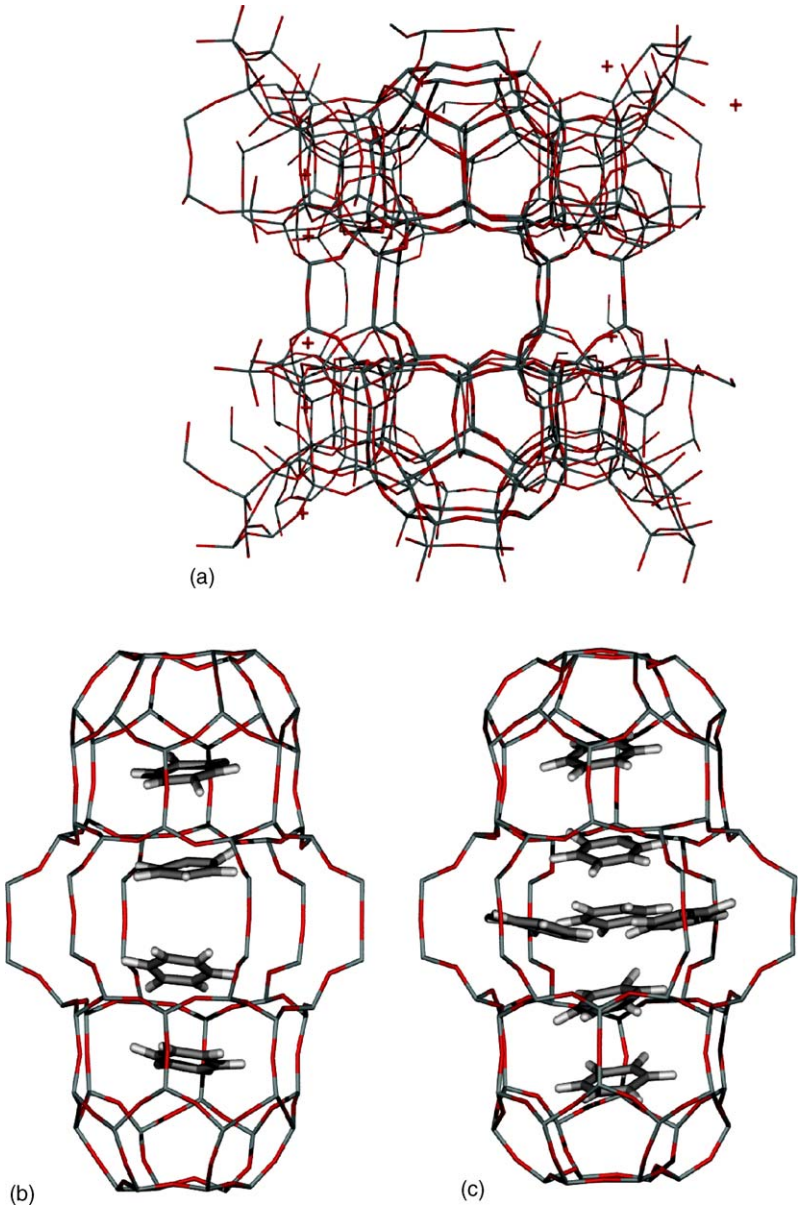

Fig. 3. Schematic view of: (a) the structure of MCM-22 zeolites showing the supercage consisting of the large cavities of 12-MR in cross-section size interconnected through short 10-MR conduits. Each large cavity consists of six 10-MR windows which form the intercage region and of two hemicages in which an energy minimum is found; (b) a snapshot of the distribution of four benzene initial molecules in one 12-MR supercage; (c) a snapshot of the distribution of benzene molecules at loadings of eight molecules (seven benzene molecules are accommodated in the supercage).

The complete sets of parameters for the potential energy functions are given in Tables 2–4.

The intramolecular potential energy of the benzene molecule is taken from the work of Sastre et al. [21]. It consists of five terms for bond stretching, bending, and torsion as well as van der Waals (vdW) and Coulomb terms:

$$V_{\text{benzene}} = V_{\text{bond-stretch}} + V_{\text{bond-bend}} + V_{\text{torsion}} + V_{\text{vdW}} + V_{\text{coul}} \quad (2)$$

Bond stretching and bending terms are modeled by harmonic potentials. The torsion potential is represented by a harmonic cosine function. The van der Waals interactions are described by a Lennard–Jones potential (Table 1).

The benzene–benzene and zeolite–benzene interactions are described by Lennard–Jones plus Coulomb terms:

$$V_{\text{benzene-benzene}} = V_{\text{Lennard-Jones}} + V_{\text{coul}} \quad (3)$$

$$V_{\text{zeolite-benzene}} = V_{\text{Lennard-Jones}} + V_{\text{coul}} \quad (4)$$

The zeolite–benzene potential consists of the Lennard–Jones and Coulombic terms describing the C–Si, C–O, H–Si, and H–O interactions. The Lennard–Jones parameters of these terms were obtained by applying the Lorentz–Barthelot combination rules:

$$\varepsilon_{ij} = \sqrt{\varepsilon_i \varepsilon_j} \quad (5)$$

Table 2
Potential parameters used for siliceous FAU (see equations in Table 1)

Two-body parameters	
Si–O	
k (kcal/mol)	597.32
r_0 (Å)	1.605
Three-body parameters	
O–Si–O	
k (kcal/mol)	138.12
θ_0 (°)	109.5
Si–O–Si	
k (kcal/mol)	10.85
k' (kcal/mol)	−34.08
k'' (kcal/mol)	26.52
θ_0 (°)	143.7

Table 3
Potential parameters used for siliceous ZSM-5 (see equations from Table 1)

Two-body parameters	
Si–O	
k (kcal/mol)	597.32
r_0 (Å)	1.591
Three-body parameters	
O–Si–O	
k (kcal/mol)	138.12
θ_0 (°)	109.5
Si–O–Si	
k (kcal/mol)	10.85
k' (kcal/mol)	−34.08
k'' (kcal/mol)	26.52
θ_0 (°)	155.9

$$\sigma_{ij} = \frac{\sigma_i + \sigma_j}{2} \quad (6)$$

We adjusted the ε parameter of the Lennard–Jones term of the C–Si, C–O, H–Si, and H–O interactions to reproduce the heat of adsorption of benzene in siliceous FAU, ZSM-5, and MCM-22 zeolites which otherwise comes out too small. This was done iteratively by changing its value and performing a test simulation until the adsorption energy resulting from the simulations was close to the experimental values (−10.71 and −13.76 kcal/mol for FAU and ZSM-5, respectively). The simulated adsorption energy was simply approximated as the average of the total potential energy over the trajectory. The parameters of the benzene–benzene and zeolite–benzene interactions are reported in Tables 5 and 6. For the zeolite atoms O and Si, partial charges of −1.0, +2.0 are taken as well as +0.153 and −0.153 for H and C of benzene.

Table 4
Potential parameters used for siliceous MCM-22 (see equations from Table 1)

Two-body parameters	
Si–O	
k (kcal/mol)	597.32
r_0 (Å)	1.605
Three-body parameters	
O–Si–O	
k (kcal/mol)	138.12
θ_0 (°)	109.5
Si–O–Si	
k (kcal/mol)	10.85
k' (kcal/mol)	−34.08
k'' (kcal/mol)	26.52
θ_0 (°)	154.8

2.3. Details of the simulation

The MD simulations were performed within the NVE ensemble at room temperature (300 K). We used the computer program DL_POLY 2.0 [22] on a Linux workstation. Initial velocities were assigned to all atoms according to a Maxwell–Boltzmann distribution corresponding to the temperature of the system. Newton's equation of motion was integrated using the Verlet algorithm with a time step of 1 fs. The electrostatic interactions were calculated by Ewald summation while the van der Waals interactions were evaluated within a cut-off radius of 12.0, 9.5, and 12.0 Å for siliceous FAU, ZSM-5, and MCM-22, respectively.

The starting configurations of the zeolite–benzene systems were relaxed by an optimization procedure consisting of a low-temperature simulation in the NPT ensemble before equilibrating for 100 ps in an NVE ensemble to reach room temperature by rescaling the velocities. Before collecting the trajectories, the system was allowed to equilibrate for 50 ps without velocity

Table 5
Potential parameters used for benzene molecules with siliceous FAU (see equations from Table 1)

	k (kcal/mol)		r_0 (Å)
Two-body parameters			
C–C	938.00		1.385
C–H	680.00		1.085
	k (kcal/mol)		θ_0 (°)
Three-body parameters			
C–C–C	126.00		120.0
C–C–H	70.00		120.0
	A	m	δ
Four-body parameters			
C–C–C–C	3.6250	2.000	180.0
C–C–C–H	3.6250	2.000	180.0
	ε (kcal/mol)		σ (Å)
Lennard–Jones parameters			
C–C	0.0860		3.400
C–H	0.0359		3.367
H–H	0.0150		2.918
C–Si	0.0418		3.570
H–Si	0.0174		3.176
C–O	0.0762		3.170
H–O	0.0318		2.770

Table 6
Potential parameters used for benzene molecules with siliceous ZSM-5 and MCM-22 (see equations from Table 1)

	k (kcal/mol)		r_0 (Å)
Two-body parameters			
C–C	938.00		1.385
C–H	680.00		1.085
	k (kcal/mol)		θ_0 (°)
Three-body parameters			
C–C–C	126.00		120.0
C–C–H	70.00		120.0
	A	m	δ
Four-body parameters			
C–C–C–C	3.6250	2.000	180.0
C–C–C–H	3.6250	2.000	180.0
	ε (kcal/mol)		σ (Å)
Lennard–Jones parameters			
C–C	0.0860		3.400
C–H	0.0359		3.367
H–H	0.0150		2.918
C–Si	0.0393		3.570
H–Si	0.0164		3.176
C–O	0.0717		3.170
H–O	0.0299		2.770

rescaling and its temperature remained constant at about 300 K. Then a 100 ps production run in the NVE ensemble was started in which the coordinates and velocities of the atoms were stored every 10 fs for subsequent analysis.

3. Results and discussion

3.1. Structures of siliceous zeolite frameworks

We calculated the intramolecular Si–Si, Si–O and O–O radial pair distribution functions (RDF) of the zeolites (Fig. 4). The maxima of the RDFs are shown in Table 7. The Si–O–Si and O–Si–O angular distribution functions are presented in Fig. 5 and the values of their maxima are also given in Table 7. Since the values from the RDF function compare well with next-neighbor distances derived from structural data of siliceous zeolites [23–25] and the probability maxima for the angles are consistent with the structural data, we can assume that this force field deals trustworthily with the geometry and small-amplitude motions of the zeolites.

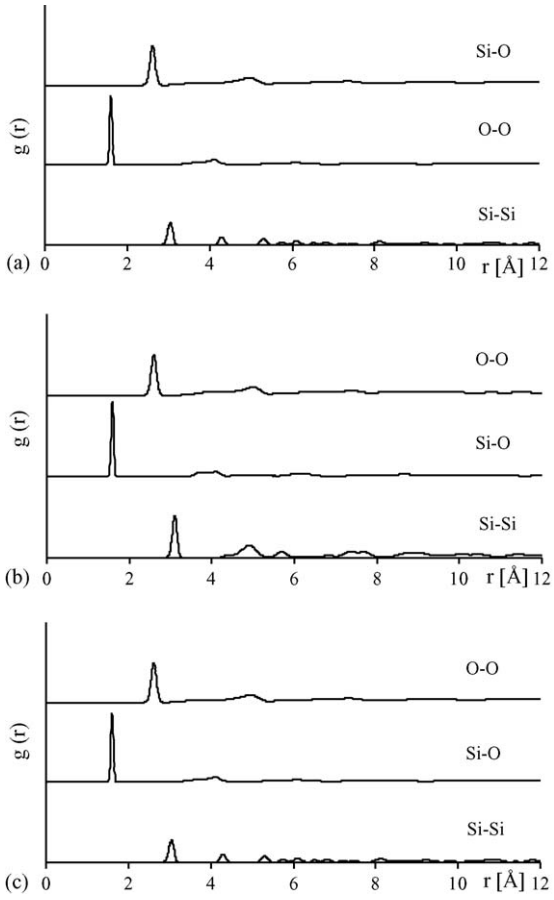

Fig. 4. Radial pair distribution functions of the Si–Si, Si–O, and O–O interatomic distances for: (a) siliceous FAU, (b) siliceous ZSM-5, and (c) siliceous MCM-22.

3.2. Adsorption energy

Table 8 reports the adsorption energies taken as an average from the configurations after the equilibration period. At the zero coverage limit (one molecule of benzene per supercell) adsorption energies of −10.81, −13.79, and −11.47 kcal/mol, are obtained for siliceous FAU, ZSM-5, and MCM-22, respectively. These values compare well with the experimental results of Jaenchen et al. [26] where heats of adsorption of

Table 7
Structural parameters (maxima of the RDF functions and of the angular probability functions) for various siliceous zeolites

Parameters	Siliceous FAU		Siliceous ZSM-5		Siliceous MCM-22	
	Simulation	Experiment [23]	Simulation	Experiment [24]	Simulation	Experiment [25]
Si–Si	3.047	–	3.102	–	3.135	–
Si–O	1.606	1.614	1.584	1.584	1.606	1.610
O–O	2.629	–	2.585	–	2.618	–
∠Si–O–Si	142.1	142.0	155.6	156.2	145.6	145.8
∠O–Si–O	109.5	109.5	109.5	109.5	109.5	109.5

Bond lengths in Å and bond angles in (°) (see text for explanation).

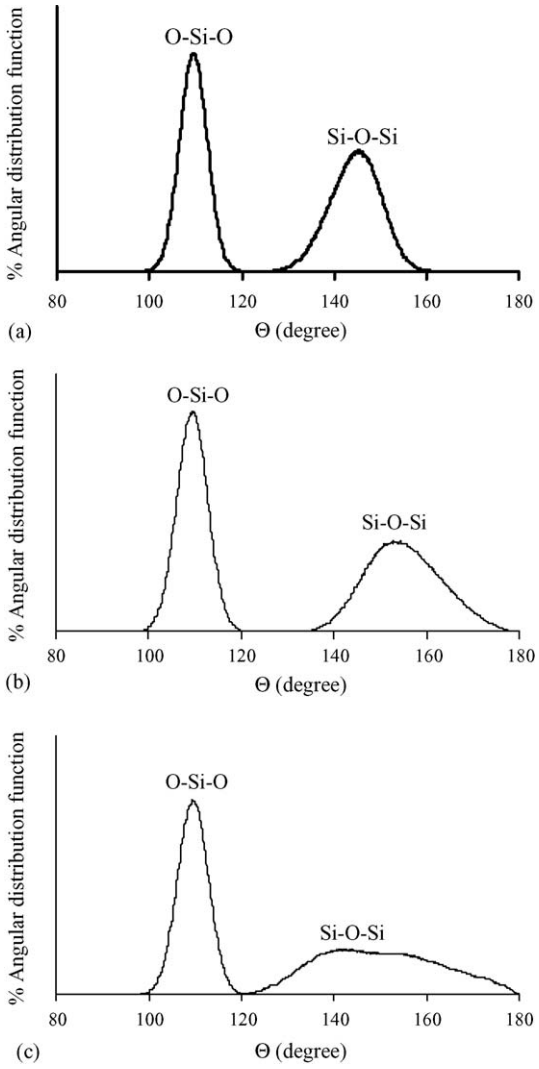

Fig. 5. Si–O–Si and O–Si–O angular distribution functions for: (a) siliceous FAU, (b) siliceous ZSM-5, and (c) siliceous MCM-22.

−10.71 and −13.76 kcal/mol are obtained for siliceous FAU and ZSM-5, respectively. This indicates that the intermolecular potential functions used here might be of reasonable quality as well.

The adsorption of aromatic hydrocarbons in zeolites is expected to result mainly from weak interaction of the π-electrons of the aromatic molecule with the terminal silanol (Si–OH) groups [27] for which no separate explicit terms are provided in our model potentials. However, since our fitting procedure tries to reproduce the experimental heat of adsorption, the Lennard–Jones parameters are adjusted to account, at least partially, for these interactions. The comparison of the adsorption energies of benzene in various siliceous zeolites shows that the difference in interaction energies of benzene in siliceous FAU, ZSM-5, and MCM-22 is related to the degree of confinement of benzene in the zeolites. Due to the smaller pore size of ZSM-5 (540 pm) than that of MCM-22 (710 pm) and FAU (740 pm) for the cage window and (1250 pm) for the supercage, the confinement effect (mainly van der Waals interactions) is stronger in siliceous ZSM-5. Since the van der Waals interactions dominate the adsorption of non-polar molecules, the adsorption energy of benzene in siliceous ZSM-5 is higher than those of siliceous MCM-22 and FAU [28].

The adsorption energies of benzene/siliceous zeolite complexes increase with increasing loading number, due to the intermolecular attraction between benzene molecules. Dispersion energy is the main component in these weak complexes.

3.3. Self-diffusion coefficients of benzene

Sorbate self-diffusion coefficients can be calculated from the mean square displacements (MSD) using the Einstein relation:

$$\langle X^2(t)\rangle = 6Dt + B \tag{7}$$

where $X^2(t)$ is the mean square displacement at time t, D is the self-diffusion coefficient, and B is the thermal factor arising from atomic vibrations. Fig. 6 shows the MSD of the center of mass of the benzene molecules for different loadings plotted as a function of time. The slope of the curves in Fig. 6 can be used to calculate the self-diffusion coefficients which are reported in Table 8. The self-diffusion coefficient of benzene in siliceous zeolites decreases with increasing loading due to the steric hindrance ('friction') between sorbates molecules passing each other. It can also be seen that the self-diffusion coefficient decreases with increasing the adsorption energy. This is not surprising, since an increased interaction between sorbate and siliceous zeolite will cause the sorbate molecule to remain at a given position of the zeolite rather than to move away from it.

The diffusion coefficient of benzene in siliceous FAU has been determined from ^{2}H NMR spin–lattice relaxation

Table 8
Adsorption energies of benzene in various siliceous zeolites and self-diffusion coefficients at different benzene loadings

Molecule(s)/supercell	Siliceous FAU		Siliceous ZSM-5		Siliceous MCM-22	
	ΔE_{Ads}[a] (kcal/mol)	D (cm^2/s)	ΔE_{Ads}[a] (kcal/mol)	D (cm^2/s)	ΔE_{Ads} (kcal/mol)	D (cm^2/s)
1	−10.81	–	−13.79	–	−11.47	–
2	−10.04	9.55×10^{-5}	−13.60	2.50×10^{-6}	−11.39	2.85×10^{-5}
4	−10.46	7.24×10^{-5}	−14.30	1.93×10^{-6}	−12.18	1.70×10^{-5}
8	−10.39	7.02×10^{-5}	−13.51	1.68×10^{-6}	−12.30	0.63×10^{-5}
16	−10.67	3.85×10^{-5}	−14.03	1.65×10^{-6}	−11.86	0.39×10^{-5}

[a] ΔE_{Ads} from experiments are −10.71 kcal/mol for siliceous FAU, and −13.76 kcal/mol for siliceous ZSM-5.

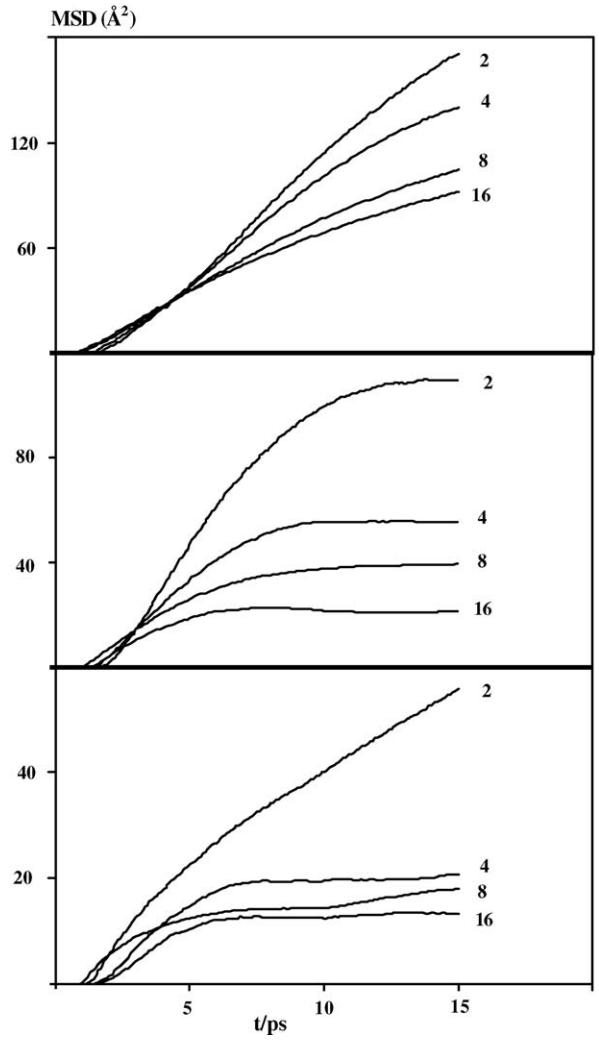

Fig. 6. Mean square displacements (MSDs) of the centers of mass of the benzene molecules in: (a) siliceous FAU, (b) siliceous ZSM-5, and (c) siliceous MCM-22 at different loadings.

experiments [$D^{298} = (4.5 \pm 3.3) \times 10^{-6}$ cm^2/s] [29]. Our self-diffusion coefficients of benzene in siliceous FAU from MD simulations in Table 8 are in good agreement with this experimental result. The self-diffusion coefficients of benzene in siliceous ZSM-5 in Table 8 compare well with the diffusion coefficient of *p*-xylene in silicalite from molecular dynamics simulations (4.08×10^{-5} cm^2/s) [30]. For siliceous MCM-22, the self-diffusion coefficients (Table 8) are in good agreement with the molecular dynamics simulations of Sastre et al. [31] (4.62×10^{-6} cm^2/s), for the diffusion coefficient of benzene in 12-MR supercages of siliceous MCM-22.

3.4. Radial distribution functions

Analysis of the radial distribution functions (RDFs) $g_{AB}(r)$ yields information about positions and structural characteristics of sorbates in the pore of zeolites. The radial distribution function is defined as the probability that two centers, A and B, are separated by a distance r:

$$g_{AB}(r) = \left\langle \frac{dn_{AB}}{dr} \frac{1}{4\pi r^2 \rho_B N_A} \right\rangle \quad (8)$$

N_A describes the number of A centers, ρ_B is the macroscopic density of the B centers, and n_{AB} is the number of AB pairs.

Fig. 7 shows the RDFs for various siliceous zeolites with different benzene loadings. We note that the benzene molecules are relatively far from each other (about 5.2 Å for siliceous FAU, 5.2 Å for siliceous ZSM-5, and 4.8 Å for siliceous MCM-22). One can see that the position of the first maximum of RDFs does not change whether there are two or three molecules of benzene present. The fact that the RDF does not reach zero after the first maximum agrees with the diffusion of the benzene molecules discussed above. It is interesting to see that the center-of-mass RDFs of benzene in the three zeolites at 300 K (Figs. 1–3) are obviously different and that the radial distribution function of diffusing molecules can be related to the structure of its nanoporous host.

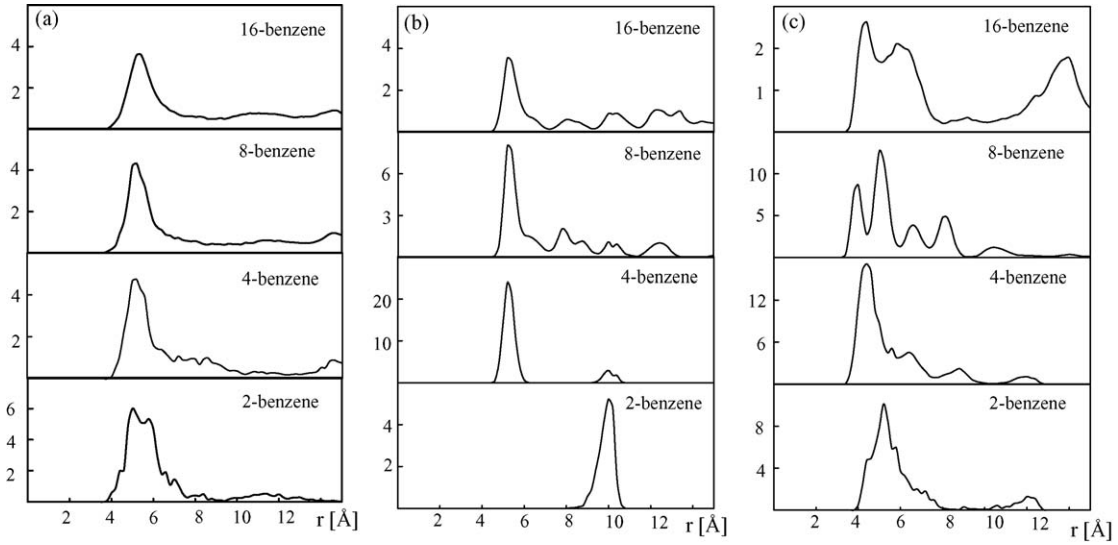

Fig. 7. Radial distribution functions of benzene in: (a) siliceous FAU, (b) siliceous ZSM-5, and (c) siliceous MCM-22 at different loadings.

For all four loadings of FAU, the first peak has its maximum at about 5.2 Å (Fig. 7a) and corresponds to a contact benzene dimer. A graphical analysis of these configurations reveals a range of distorted V-shaped structures. Fig. 1b shows a snapshot of a typical configuration of four benzene molecules in one supercage of FAU. The benzene molecules prefer to be adsorbed parallel to the surface of the sodalite cage above the six-membered-ring. The height of the peak maximum in the RDF decreases with loading, and is shifted toward larger distances, indicating an increasing disorder between the benzene molecules.

In ZSM-5, the position of the first maximum in the RDF (Fig. 7b) is at about the same distance as found in FAU. However, the conformation of the benzene molecule is different to each other. A T-structure [32,33] where the planes of the aromatic rings are perpendicular was frequently found in this zeolite at loadings of 2, 4, and 8 molecules per supercell. Fig. 2b shows a snapshot of this T-structure. At loadings of 16 molecules per supercell we found the benzene molecules in the straight channel to be stacked parallel to each other (Fig. 2c). This configuration, including some roughly ''parallel stacked and displaced'' structure is also observed at loadings of 16 molecules per supercell where the movement of the molecules is also highly correlated. This behavior may be responsible for the clustered diffusion reported by Song et al. [34]. The RDF data at loadings of 2 and 4 molecules per supercell show two maxima of which the first one (at about 5 Å) corresponds to benzene molecules adsorbed in the intersecting channel and in the straight channel, while the second one (at about 10 Å) corresponds to two benzene molecules adsorbed in two neighboring intersecting channels. At loadings of 8 and 16 molecules per supercell, two smaller peaks appear at about 8 and 12 Å, which correspond to the neighboring benzene molecule adsorbed in the zigzag channel and in the other intersecting channel connected to the zigzag channel, respectively. These results agree well with the distances of the interconnecting channel system in the ZSM-5 framework.

The positions of the first maxima found in MCM-22 are different from those in FAU and in ZSM-5. At a loading of 2, the RDF maximum is found at about 5 Å. It appears to at about 4 Å at a loading of 4 and their orientation of the benzene molecules is similar to the stacked conformation (Fig. 3b) of benzene dimer in the gas phase [32,33]. This configuration is found also at a loading of 2 molecules per supercage when starting with benzene dimers located at the S2 sites above and below the central part of the 12-MR supercages. It is found as well at higher loadings when benzene molecules are located at the S2 and S3 sites which consist of large 12-MR supercages interconnected with 10-MR windows. The benzene dimer still exists throughout the simulation run. In the simulation with eight benzene molecules the supercage is already saturated. After the equilibration period, only seven benzene molecules are accommodated in the supercage (Fig. 3c) three in the middle near the 12-membered rings and four only in the cylindrical volume above and below. Since the cylindrical volume of the supercage is about 720 $Å^3$, each of the four benzene molecules occupies a volume similar to the one in liquid benzene. Therefore, it is not unreasonable that this loading is indeed close to the saturation limit. Similar values were found or discussed in previous works [34–37].

4. Conclusions

We have performed molecular dynamics simulations of the siliceous zeolites FAU, ZSM-5 and MCM-22 with 2, 4, 8 and 16 benzene molecules. The potential energy functions for these simulations were constructed in a semi-empirical way from existing potentials and experimental energetic data. We calculated the zeolite–benzene radial distribution functions and found the benzene molecules relatively far from each other, at distances of about 5.2 Å for siliceous FAU, 5.2 Å for siliceous ZSM-5 and 4.8 Å for siliceous MCM-22. The diffusional behavior shows that in ZSM-5 zeolite–benzene molecules cannot leave the original cage whereas in the other two zeolites they can diffuse out of it. In the case of FAU the benzene molecules prefer to be adsorbed parallel to the surface of the sodalite cage above the six-membered-ring. In ZSM-5, we found a T-structure of benzene molecules at a loading of 2, 4, and 8 molecules per supercell. At loadings of 16 molecules per supercell, the molecules are lined up parallel to each other along the straight channel and their movement is highly correlated. Finally, in the case of MCM-22 at a loading of 4, adjacent benzene molecules assume an orientation similar to the stacked conformation of benzene dimer in gas phase [32,33].

Acknowledgements

This work was supported in part by grants from the Thailand Research Fund (TRF Senior Research Scholar to JL), the Center of Nanotechnology, Kasetsart University Research and Development Institute, and the Kasetsart University Research and Development Institute (KURDI), as well as the Ministry of University Affairs under the Science and Technology Higher Education Development Project (MUA-ADB funds). Support from the National Nanotechnology Center (Thailand) and the Dow Chemical Company (USA) are also acknowledged.

References

[1] R.A. van Santen, G.J. Kramer, Reactivity theory of zeolitic broensted acidic sites, Chem. Rev. 95 (1995) 637–660.
[2] C.R.A. Catlow, Modeling of Structure and Reactivity in Zeolites, Academic Press, San Diego, 1992.
[3] R. Roque-Malherbe, R. Wendelbo, A. Mifsud, A. Corma, Diffusion of aromatic hydrocarbons in H-ZSM-5, H-Beta, and H-MCM-22 zeolites, J. Phys. Chem. 99 (1995) 14064–14071.
[4] J. Perez-Pariente, E. Sastre, V. Fornes, J.A. Martens, P.A. Jacobs, A. Corma, Isomerization and disproportionation of *m*-xylene over zeolite b, Appl. Catal. 69 (1991) 125–137.
[5] U. Sridevi, B.K.B. Rao, N.C. Pradhan, S.S. Tambe, C.V. Satyanarayana, B.S. Rao, Kinetics of isopropylation of benzene over HBeta catalyst, Ind. Eng. Chem. Res. 40 (2001) 3133–3138.
[6] C. Ercan, F.M. Dautzenberg, C.Y. Yeh, H.E. Barner, Mass-transfer effects in liquid-phase alkylation of benzene with zeolite catalysts, Ind. Eng. Chem. Res. 37 (1998) 1724–1728.

[7] A. Corma, C. Corell, A. Martinez, J. Perez-Pariente, Insight into the pore structure of zeolite MCM-22 through catalytic tests, Stud. Surf. Sci. Catal. 84 (1994) 859–866.
[8] S. Unverricht, M. Hunger, S. Ernst, H.G. Karge, J. Weitkamp, Zeolite MCM-22: synthesis, de-alumination and structural characterization, Stud. Surf. Sci. Catal. 84 (1994) 37–44.
[9] R. Ravishankar, T. Sen, V. Ramaswamy, H.S. Soni, S. Ganapathy, S. Sivasanker, Synthesis, characterization and catalytic properties of zeolite PSH-3/MCM-22, Stud. Surf. Sci. Catal. 84 (1994) 331–338.
[10] P. Demontis, E.S. Fois, G.B. Suffritti, S. Quartieri, Molecular dynamics studies on zeolites. 4. Diffusion of methane in silicalite, J. Phys. Chem. 94 (1990) 4329–4334.
[11] R.L. June, A.T. Bell, D.N. Theodorou, Molecular dynamics studies of butane and hexane in silicalite, J. Phys. Chem. 96 (1992) 1051–1060.
[12] S. Yashonath, J.M. Thomas, A.K. Nowak, A.K. Cheetham, The siting, energetics and mobility of saturated hydrocarbons inside zeolitic cages: methane in zeolite Y, Nature 331 (1988) 601–604.
[13] V.A. Ermoshin, K.S. Smirnov, D. Bougeard, Ab initio generalized valence force field for zeolite modelling. 2. Aluminosilicates, Chem. Phys. 209 (1996) 41–51.
[14] D.H. Olson, Crystal structure of the zeolite nickel faujasite, J. Phys. Chem. 72 (1968) 4366–4373.
[15] A.N. Fitch, H. Jobic, A. Renouprez, Localization of benzene in sodium-Y-zeolite by powder neutron diffraction, J. Phys. Chem. 90 (1986) 1311–1318.
[16] H. Klein, H. Fuess, G. Schrimpf, Mobility of aromatic molecules in zeolite NaY by molecular dynamics simulation, J. Phys. Chem. 100 (1996) 11101–11112.
[17] G.J. Kennedy, S.L. Lawton, M.K. Rubin, 29Si MAS NMR studies of a high silica form of the novel molecular sieve: MCM-22, J. Am. Chem. Soc. 116 (1994) 11000–11003.
[18] M.E. Leonowicz, J.A. Lawton, S.L. Lawton, M.K. Rubin, MCM-22: a molecular sieve with two independent multidimensional channel systems, Science 264 (1994) 1910–1913.
[19] J.B. Nicholas, A.J. Hopfinger, F.R. Trouw, L.E. Iton, Molecular modeling of zeolite structure. 2. Structure and dynamics of silica sodalite and silicate force field, J. Am. Chem. Soc. 113 (1991) 4792–4800.
[20] K.S. Smirnov, D. Bougeard, Molecular dynamics study of the vibrational spectra of siliceous zeolites built from sodalite cages, J. Phys. Chem. 97 (1993) 9434–9440.
[21] G. Sastre, N. Raj, C.R.A. Catlow, R. Roque-Malherbe, A. Corma, Selective diffusion of C8 aromatics in a 10 and 12 MR zeolite. A molecular dynamics study, J. Phys. Chem. B 102 (1998) 3198–3209.
[22] W. Smith, T.R. Forester, The DLPOLY 2.0 User Manual, CCLRC, Daresbury Laboratory, 1995.
[23] M. Colligan, P.M. Forster, A.K. Cheetham, Y. Lee, T. Vogt, J.A. Hriljac, Synchrotron X-ray powder diffraction and computational investigation of purely siliceous zeolite Y under pressure, J. Am. Chem. Soc. 126 (2004) 12015–12022.
[24] S. Nair, M. Tsapatsis, The location of *o*- and *m*-xylene in silicalite by powder X-ray diffraction, J. Phys. Chem. B 104 (2000) 8982–8988.
[25] M.A. Camblor, A. Corma, M.-J. Diaz-Cabanas, C. Baerlocher, Synthesis and structural characterization of MWW type zeolite ITQ-1, the pure silica analog of MCM-22 and SSZ-25, J. Phys. Chem. B 102 (1998) 44–51.
[26] J. Jaenchen, H. Stach, L. Uytterhoeven, W.J. Mortier, Influence of the framework density and the effective electronegativity of silica and aluminophosphate molecular sieves on the heat of adsorption of nonpolar molecules, J. Phys. Chem. 100 (1996) 12489–12493.
[27] A. Jentys, N.H. Pham, H. Vinek, Nature of hydroxy groups in MCM-41, J. Chem. Soc., Faraday Trans. 92 (1996) 3287–3291.
[28] R. Rungsirisakun, B. Jansang, P. Pantu, J. Limtrakul, The adsorption of benzene on industrially important nanostructured catalysts (H-BEA, H-ZSM-5, and H-FAU): confinement effects, J. Mol. Struct. 733 (2004) 239–246.
[29] L.M. Bull, N.J. Henson, A.K. Cheetham, J.M. Newsam, S.J. Heyes, Behavior of benzene in siliceous faujasite: a comparative study by ^{2}H NMR and molecular dynamics, J. Phys. Chem. 97 (1993) 11776–11780.
[30] F.J. Llopis, G. Sastre, A. Corma, Xylene isomerization and aromatic alkylation in zeolites NU-87, SSZ-33, Beta, and ZSM-5: molecular dynamics and catalytic studies, J. Catal. 227 (2004) 227–241.
[31] G. Sastre, C.R.A. Catlow, A. Corma, Diffusion of benzene and propylene in MCM-22 zeolite. A molecular dynamics study, J. Phys. Chem. B 103 (1999) 5187–5196.
[32] W.L. Jorgensen, D.L. Severance, Aromatic–aromatic interactions: free energy profiles for the benzene dimer in water, chloroform, and liquid benzene, J. Am. Chem. Soc. 112 (1990) 4768–4774.
[33] M.O. Sinnokrot, C.D. Sherrill, Highly accurate coupled cluster potential energy curves for the benzene dimer: sandwich, T-shaped, and parallel-displaced configurations, J. Phys. Chem. A 108 (2004) 10200–10207.
[34] L. Song, Z.-L. Sun, H.-Y. Ban, M. Dai, L.V.C. Rees, Studies of unusual adsorption and diffusion behavior of benzene in silicalite-1, Phys. Chem. Chem. Phys. 6 (2004) 4722–4731.
[35] R.L. Portsmouth, M.J. Duer, L.F. Gladden, ^{2}H NMR studies of single-component adsorption in silicalite: a comparative study of benzene and *p*-xylene, J. Chem. Soc., Faraday Trans. 91 (1995) 559–567.
[36] B.F. Mentzen, F. Lefebvre, Flexibility of the MFI silicalite framework upon benzene adsorption at higher pore-fillings: a study by X-ray powder diffraction, NMR and molecular mechanics, Mater. Res. Bull. 32 (1997) 813–821.
[37] A. Sahasrabudhe, V.S. Kamble, A.K. Tripathi, N.M. Gupta, FTIR study on molecular motions of benzene adsorbed in ZSM-5 zeolite: role of charge-balancing cations and pore size, J. Phys. Chem. B 105 (2001) 4374–4379.